A Ka-band Doppler Scatterometer for the Simultaneous Measurement of Ocean Surface Vector Winds and Currents

Alexander Wineteer, Dragana Perkovic-Martin, Raquel Monje, Ernesto Rodríguez, Tamas Gál, Noppasin Niamsuwan, Fabien Nicaise, Karthik Srinivasan, Chad Baldi, Ninoslav Majurec, and Bryan Stiles

Jet Propulsion Laboratory, California Institute of Technology

***Abstract*—Ocean surface currents and winds are closely coupled, essential climate variables, and synoptic measurements of them over large areas presents a problem that must be tackled with remote sensing techniques. DopplerScatt is a spinning, Ka-band Doppler Scatterometer capable of simultaneous measurements of ocean vector winds and currents over a wide 25 km swath at 200 m pixel resolution. The synoptic scale and very high resolution attained by DopplerScatt enable the study of submesoscale ocean currents and winds, their interactions, and the computation of their derivative fields. DopplerScatt was initially developed under funding from the NASA Instrument Incubator program, and is currently being made field-ready under the NASA Airborne Instrument Technology Transition program. Here, we will present the measurement principle behind Doppler Scatterometry and summarize the hardware, performance, and validation of the DopplerScatt instrument, along with a short section on operating the instrument.**

I. Introduction

At large scales, ocean currents play an important role in governing global climate balance and weather, including the dynamics of El Niño and the Pacific Decadal Oscillation. At smaller meso- and submesoscales, ocean surface currents play a significant role in the dissipation of energy in the ocean [1], pollution dispersion (e.g., oil spills), ocean biology (via nutrient and phytoplankton advection and up/downwelling) [2], and coastal shipping.

The significance of ocean currents for NASA was demonstrated in the selection of the Surface Water and Ocean Topography mission. SWOT's measurement of ocean topography allows for the estimation of the geostrophic component of the current associated with sea surface height anomalies. However, SWOT will not be able to capture ageostrophic currents, which account for about 75 percent of the kinetic energy transfer between the ocean and atmosphere [3] [4]. More recently, the National Academy identified ocean surface currents as a targeted Explorer Class observable in their Decadal Review [5].

On the other side of the air-sea boundary layer lie ocean winds. Measurements of ocean vector winds from spaceborne scatterometers allow for global, daily estimates of surface wind speed and direction, critical to now/fore-casting weather, hurricanes, and even in ship routing. Ocean vector winds are an important variable governing the transfer of momentum, gases, and latent heat between the atmosphere and the ocean, and the details of these couplings have come to light largely due to data from scatterometers.

There is a close two-way relationship between ocean surface currents and the wind. The wind drives Ekman surface currents and Stokes drift, but surface currents also modulate wind momentum transfer through kinematic effects [6] [7], and through modulation of the air-sea boundary layer by the temperature of the water carried by the currents [8] [9]. Therefore, to fully understand the air-sea interaction mechanisms, a critical mechanism governing the Earth's climate and weather, it is important to make simultaneous estimates of both winds and surface currents.

Clearly, there is both scientific and operational merit to measuring global vector ocean surface currents from space, especially simultaneously with vector surface winds, but to date there has been no mission to do so, in large part due to necessary technology development.

The potential for measuring ocean currents from space using two antennas has been understood since the pioneering work of Goldstein et al. [10] in along-track interferometry (ATI). Spaceborne ATI current measurements of a single radial velocity component were demonstrated by Romeiser et al. [11] using SRTM data. Subsequently, Freeman et al. [12] proposed getting full vector currents by spinning the two antennas. The ATI technique, although promising greater precision, requires large antennas separated by a considerable distance (10 m) and suffers from either swath limitations (non-spinning antenna) or mechanical complexity (spinning two large antennas separated by a large mast). An approach that requires only one antenna to measure one velocity component was proposed by van der Kooij (unpublished) and refined by Chapron and coworkers [13]. This approach used the Doppler centroid (rather than interferometric phase) measured by a SAR to estimate the radial velocity along the beam direction. Chapron et al. [13] also demonstrated the need to have simultaneous vector wind estimates to enable the translation of the measured Doppler into surface currents along the look direction. Using a SAR instrument, it was not possible to obtain vector winds due to the lack of absolute calibration and the inability to retrieve direction using only one look direction.

Fig. 1: View of the NASA King Air B200 with the DopplerScatt radome mounted on the underside.

DopplerScatt enables the simultaneous measurement of vector surface currents and winds by spinning a single pencil beam. By transmitting bursts of radar pulses, successive pulse pair phase differences are used to determine surface current radial velocities in the look direction after the removal of platform motion. The return power of those same pulses is used to determine the surface backscatter as used in scatterometery to estimate wind speeds. By spinning the antenna on a moving platform, multiple views are obtained for each ground cell, enabling estimation of wind and current vectors over a wide swath [14].

Section II presents an overall description of the DopplerScatt instrument and its operating parameters, section III talks about the instrument's calibration and estimated performance, section IV discusses DopplerScatt operations, section V gives a high-level overview of data processing. In section VI we present brief results of flights to date.

II. The DopplerScatt instrument and its operating parameters

The DopplerScatt instrument is an airborne single-beam Ka-band scatterometer burst system, capable of wide ranging system parameters that can support many configurations in terms of the inter-pulse period, the burst repetition interval, and the system bandwidth. In Table I we present the configuration used to obtain the results presented in section VI. The system is deployed from a King Air B200 platform (owned and operated by NASA Armstrong Flight Research Center) at a nominal flight altitude of 8.5 km. Figure 1 and Figure 2 show a view of the aircraft with the DopplerScatt radome and the Dopplerscatt instrument in its flight configuration, respectively. The instrument is installed through a nadir-facing aircraft port, with the Ka-band transparent radome extending beneath the aircraft and the radar electronics extending into a pressure box in the aircraft cabin (Figure 6b). The pressure box that contains DopplerScatt electronics is vented to the atmosphere and allows the cabin to remain pressurized. Data from the radar passes through bulkheads on the pressure box to a operations rack inside the aircraft where it is recorded and quick-look processed in real time.

The system uses a Ka-band Solid State Power Amplifier (SSPA) built by QuinStar Technology (Torrance, CA, USA), with a peak power output of approximately 100 W, together with a 3° beamwidth antenna and a 5 MHz chirp to achieve a nominal noise-equivalent, σ_0, of about -39 dB. Upgraded hardware now allows for a 10 MHz chirp with a nominal noise-equivalent, σ_0, of about -38 dB. These levels of nominal noise-equivalent σ_0 ideally allow for sampling down to wind speeds of about 2 m/s. The antenna is a completely passive vertically polarized waveguide slot array, mechanically mounted at a nominal boresight look angle of 56°. This leads to a ground swath width of 25 km when spun about the nominal vertical axis at a rotation rate of 12.5 RPM at 8.5 km altitude. Received, base-banded data are digitized by a commercial digital receiver built by Remote Sensing Solutions (Barnstable, MA, USA), before being redundantly recorded on solid state hard drives.

Although the system pulse repetition frequency allows for SAR processing, the achievable azimuth resolution using SAR will vary significantly with azimuth angle, and, at this point, data are processed in real-aperture mode to obtain more uniform sampling characteristics. This leads to an azimuth footprint size of approximately 600 m. In the range direction, the 5 MHz chirp bandwidth results in a ground resolution of 36 m. The achievable ground resolution when combining multiple looks for different directions will vary across the swath, but can lead to significant decrease in the resolution cell size, especially in the swath "sweet-spots" between the nadir track and the far-swath.

Doppler pulse-pair processing is achieved by cross-correlating bursts which are transmitted at a burst repetition frequency of 4.5 kHz, and fully sample the Doppler bandwidth for all azimuth angles. The system's phase and power stability are monitored by a calibration loop which includes most of the transmit and receive path, aside from the rotating antenna.

The instrument position and attitude are obtained using GPS coupled with an Applanix-610 Internal Motion Unit (IMU). The rotation angle is obtained by means of an encoder, which has a nominal resolution of 88mdeg. Both the spin motor and encoder were built by Aerotech. The nominal antenna pointing is calibrated by means of nearfield antenna pattern tests and mechanical measurements of the antenna location. The accuracy of the IMU, encoder, and antenna pattern measurements is quite important to DopplerScatt since platform motion must be removed from Doppler-inferred radial velocity measurements. Any misalignment in pointing (real or due to imperfect knowledge) will project the significant airplane motion into the relatively small surface currents. We have found the Applanix-610 accuracy sufficient, and have developed methods for calibrating/correcting encoder and antenna pattern measurements that will be presented in the next section.

III. DopplerScatt calibration and estimated performance

A full system characterization of the DopplerScatt instrument was performed through a series of laboratory tests, during which the gain of the transmit chain was adjusted to ensure saturation of the SSPA, the receiver chain was tested for linearity, and the receiver noise levels were examined and

TABLE I: DopplerScatt Instrument Configuration for 5MHz Mode

Parameter	Value
Peak Power	100 W
3 dB Azimuth Beamwidth	3°
3 dB Azimuth Footprint	800 m
3 dB Elevation Beamwidth	3°
3 dB Elevation Footprint	1.4 km
Nominal boresight angle	56°
Burst Repetition Frequency	4.5 kHz
Inter-pulse Period	18.4 μsec
Chirp length	6.4 μsec
Pulses per burst	4
Pulse Bandwidth	5 MHz
Azimuth Looks	100
Range Resolution	30 m
Resolution in Elevation	36.2 m
Resolution in Azimuth	600 m
Nominal Platform Altitude	8.53 km
Nominal Swath	25 km
Scan Rate	12.5 RPM
Noise Equivalent	-37 dB

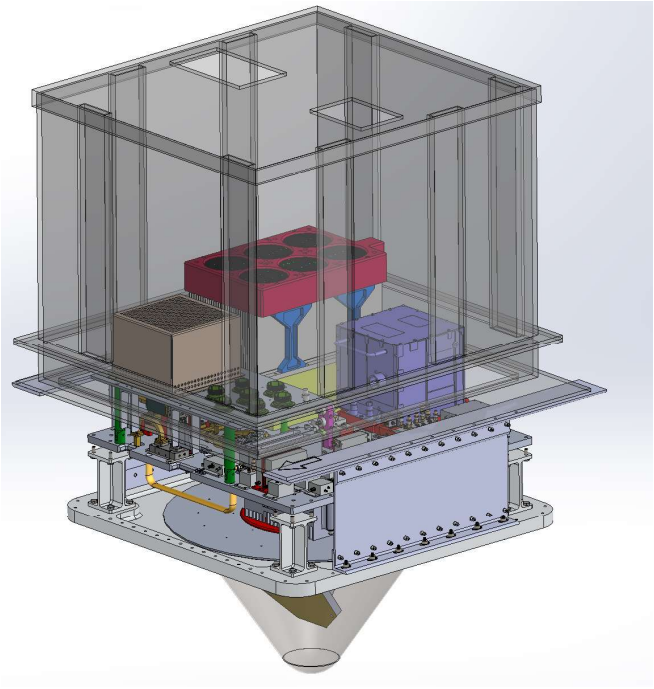

Fig. 2: The DopplerScatt instrument in its flight configuration. The instrument is easy to install in the nadir-looking aircraft port.

determined to have satisfactory performance. The system was tested as a whole over long periods of time ($\sim$ 8 hrs) where system performance was evaluated for clock drift, encoder position and spin motor velocity, temperature, and phase of calibration pulses. The system's stability of the radar master oscillator (STALO) drift over an 8 hr data collection is tracked and recorded in flight and can be evaluated in post-processing (Figure 3).

The DopplerScatt instrument has an internal calibration loop path that allows for sampling of the transmitted waveform that passes through the full receiver chain except the rotating antenna. The system records all transmitted and received pulses into the data stream on every burst (Burst Repetition Interval (BRI) $\sim$ 200 μs), including calibration pulses, which vary over time primarily due to temperature changes of the system's components. During flight, a heater is used to maintain constant component temperatures.

The radar timing and phase performance was tested using a Fiber Optic Delay Line (FODL) at the system's attenuated output. The FODL tests enable us to test delays and settings of the radar timing, while ensuring that the system's phase is stable over a data take. FODL tests were performed both with temperature control of the instrument plate (to which all of the system's components are assembled to) and without temperature control. The tests with and without thermal control concluded that temperature control in a laboratory setting does not have any influence on the differential phase of the pulses used to infer Doppler velocity. Phase differences between calibration pulses (attenuated transmit pulses routed into the receiver for tracking of transmit power and receiver gain) and delay line "echo" pulses were very stable over the collection times and their difference in standard deviation comes from the difference in SNR as shown in Figure 3. The cal pulses have a SNR of $>$ 35 dB while return pulses have $\sim$ 10 dB, depending on the wind speed. After FODL tests were completed, the output of the transmit chain was connected to the antenna which radiated into an RF hat (preventing RF leakage) to verify that there are no leakage paths in the transmit chain that could affect the calibration pulses.

Antenna gain and phase measurements were performed to characterize the antenna's base radiation pattern and its variations due to radome losses across spin angle. Figure 4 shows the variation of the antenna pattern in antenna azimuth and elevation coordinates for various radome positions. Irregularities in the radome, due to material or manufacturing, have a more noticeable effect on the azimuth pattern than on the elevation pattern. The radome induces variable changes in gain as the antenna rotates of about 0.1 dB.

In addition to calibrations done at the hardware level, DopplerScatt data was used to further refine pointing knowledge. Elevation angle was calibrated using DopplerScatt backscatter data to estimate the error in look angle knowledge by assuming the slope of the relationship between backscatter and look angle should be about -0.3 dB/degree at Ka-band [15]. Surface radial velocity data from repeat-pass lines flown in opposite directions were used to estimate the absolute error in azimuth pointing, along with the variation in azimuth pointing due to inconsistencies in either the antenna spin motor velocity or the spin encoder readings. Each of these calibrations led to significant improvements in retrieved winds and currents and have held constant under consistent radar

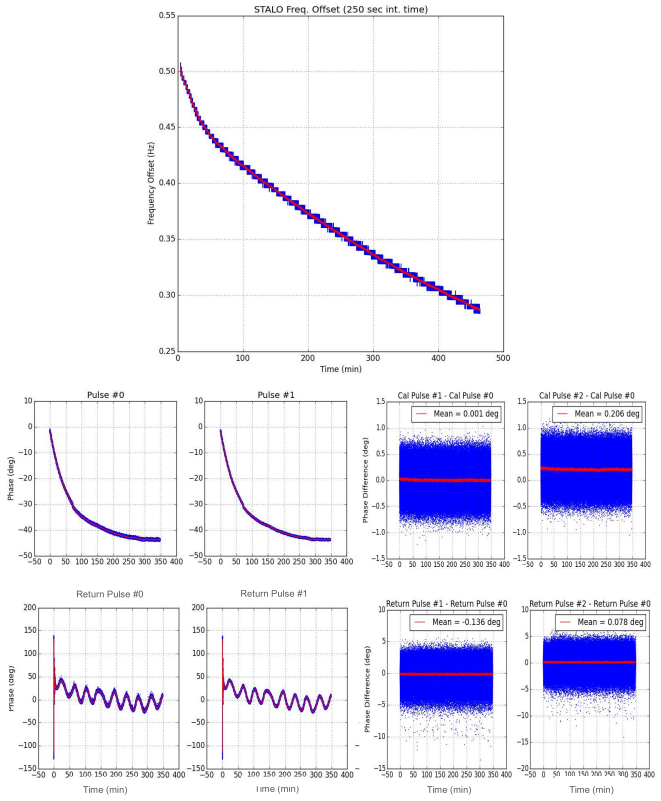

Fig. 3: Top: Drift of the 10 MHz STALO over time during lab testing. Left 4-panel: Phase variation of the calibration pulses (top) and the return pulses (bottom) from the FODL. Right 4-panel: Pulse phase difference between the calibration pulses and the return pulses.

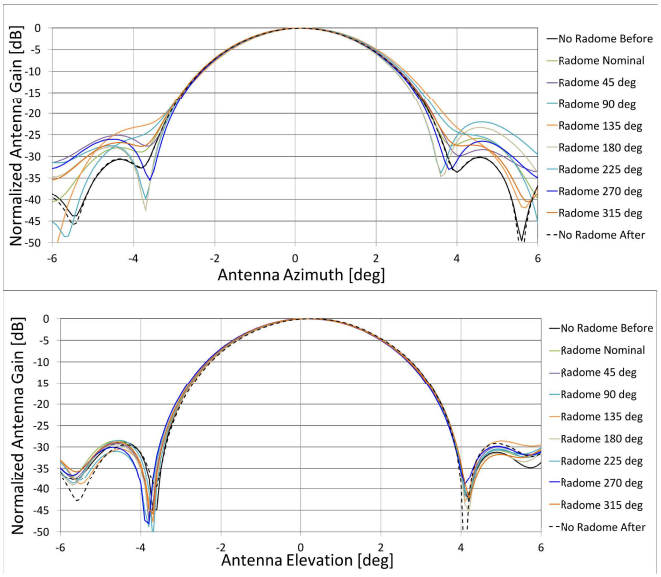

Fig. 4: Variation of the azimuth (top) and elevation (bottom) antenna pattern due to the radome with spin angle. Only the center three degrees are used in processing.

parameter settings. For more information on the data-based calibration and algorithms used in processing, see [14] for an in-depth discussion.

IV. DopplerScatt Operations

DopplerScatt is deployed from a King Air B200 aircraft owned and operated by NASA Armstrong Flight Research Center (previously deployed on a Department of Energy King Air B200). The aircraft was chosen for its relatively slow flight speed that ensures adequate antenna rotational coverage across the entire ground swath. This aircraft is capable of about five to six hours of continuous flight, typically with about an hour of takeoff and landing time; this yields maximum science data coverage of about five hours per flight. At a ground speed of about 300 km/hr, and a swath width of 25 km, DopplerScatt can measure winds and currents in an area of about 7,500 km^2/hr, or nearly 40,000 km^2 in a single flight.

DopplerScatt is operated by a single instrument operator from inside the airplane cabin. An instrumentation rack is mounted inside the aircraft (Figure 6b), and allows for all radar functions to be controlled. The instrument takes about 15 minutes to start up on the ground prior to take off, during which the instrument is checked out fully, with the exception of the SSPA, which is not turned on until a safe flight altitude is reached.

During flight, minimal operator control is required assuming nominal operation. Information on the health of the instrument, including temperatures, IMU/GPS quality, and antenna spin rate are displayed in real time for the operator. Received radar pulses and calibration pulses are displayed periodically as well. Two servers are installed on the instrumentation rack to redundantly record radar data. On one of these servers, data are processed up to backscatter and surface radial velocities, and are displayed on a map for the operator 5. From this, the operator can determine whether the instrument is collecting scientifically useful data, particularly to check if winds are high enough for data to be collected. Low winds appear as very low backscatter to the operator due to a glassy, smooth ocean surface.

After flight, data is removed on solid-state hard drives for further processing and archival. From the data processed onboard the aircraft, a quick-look vector winds and currents product can be produced on a typical computer in a couple of hours. Raw data is backed up before full (non-quick-look) processing. Full processing can be completed overnight using a custom cluster of eight Mac Mini computers. The cluster is designed to be easily portable during deployments in a standard ”carry on” sized bag. Processing on the cluster is controlled using any laptop computer over a wireless VNC.

DopplerScatt flight planning necessitates thought in a few key areas. Flight regions must be accessible: military and civilian flight restrictions may prevent transit and may interfere directly with a desired flight region. Weather plays a role in determining flights. Wind speeds at the ocean surface must be above 2-3 m/s to receive meaningful radar returns. While clouds are typically transparent at Ka-band, rain drops are not.

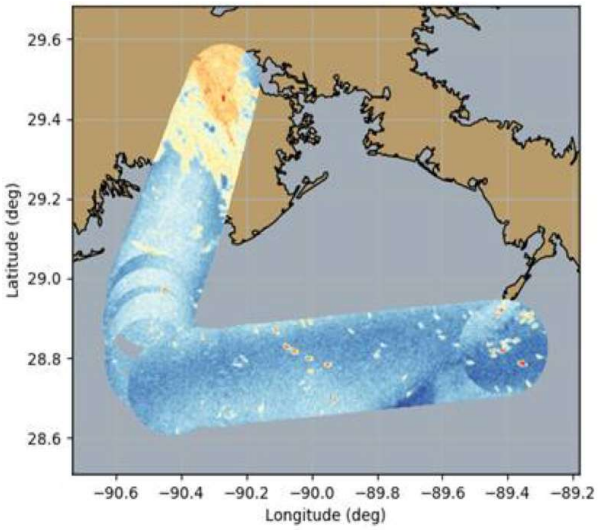

Fig. 5: DopplerScatt is capable of real-time processing onboard the aircraft and offers the operator a view of radar backscatter during the flight. This view was taken during a flight line in the Gulf of Mexico in April 2017.

Rain will contaminate data in ways we are not yet aware of because we have not flown in rainy conditions. Winds at flight altitude can push the airplane too fast for the antenna's spin rate, leading to skipping ground cells. This can be corrected by lowering the resolution of processed winds and currents, but should be avoided for the nominal 200 m resolution. A good rule of thumb is to avoid flight altitude winds of more than 80 km/hr. Finally, and perhaps obviously, consider whether there are in-situ measurements already in place that can aid in post-flight analysis and in planning flights. Using in-situ measurements, models, and DopplerScatt's own quick-look wind and current measurements can help determine the best time and place to fly during deployments.

V. Data processing overview

For a lower level, full discussion of the algorithms used to produce winds and currents from DopplerScatt, we direct the reader to Rodriguez el al. 2018 [14]. For completeness, we will briefly touch on processing here.

DopplerScatt estimates wind speeds much like any traditional scatterometer [16]. Backscatter is measured from multiple relative azimuth angles (the angle between the antenna azimuth and the wind direction) and an optimizer is used to pick the wind speed and direction that most closely fit measured backscatter to an empirically derived wind geophysical model function (wGMF). The Ka-band wGMF was developed using DopplerScatt backscatter data combined with coincident high resolution wind models from the Naval Research Laboratory Coastal Ocean/Atmosphere Mesoscale Prediction System and NOAA Seawinds. Radial surface currents are initially estimated along the ground-projected antenna look vector by using

(a)

(b)

Fig. 6: (a) DopplerScatt engineers Raquel Monje and Fabien Nicaise installing the instrument into the NASA King Air B200 instrument port. Photo Credit: Ken Ulbrich, NASA AFRC(b) DopplerScatt operator Alex Wineteer in fight monitoring instrument health and incoming backscatter data, seated in front of the instrumentation rack. Photo Credit: Carla Thomas, NASA AFRC

pulse-pair phase differences. Multiple observations of each ground cell allow radial surface currents to be combined into a vector measurement. These initial surface currents include a significant component related not to the true surface current, but to the propagation of the centimeter-scale wind-driven capillary waves that Ka-band radars interact with. An empirical current geophysical model function (cGMF) is used to remove this contamination, using the DopplerScatt winds as an input. The DopplerScatt cGMF was initially developed assuming only wind-driven currents and subsequently tuned with HF radar data taken off the coasts of Oregon and California.

VI. High level results from DopplerScatt campaigns

DopplerScatt has been flown in campaigns near the outlet of the Columbia river, along Big Sur, off the coast of San Francisco, near Monterey Bay, and twice in the Gulf of

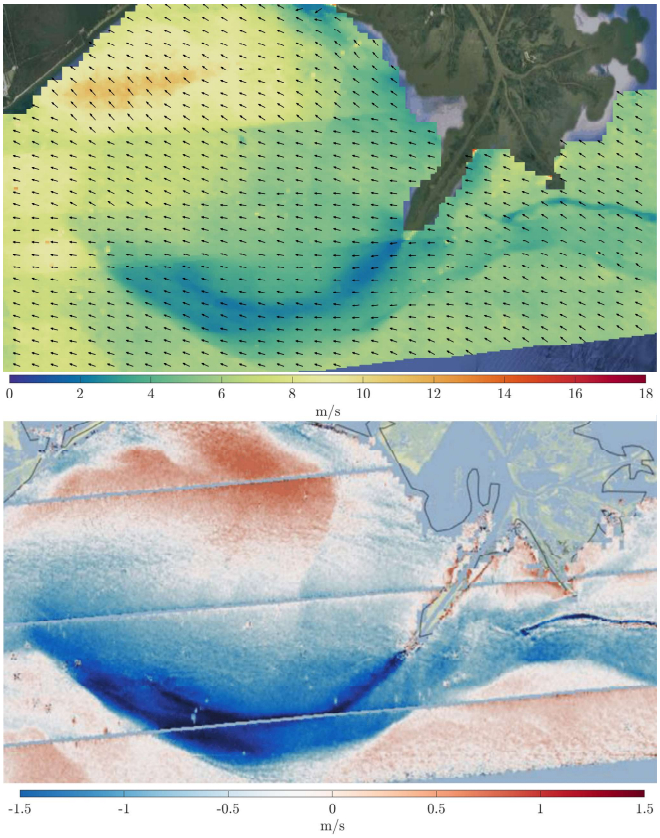

Fig. 7: Top: Wind vectors as measured by DopplerScatt in April of 2017 near the outlet of the Mississippi river, in the gulf of Mexico. Bottom: U (East-West) component of vector surface currents as measured by DopplerScatt in the same region.

Mexico. In each case, wind and current vector fields were processed and compared to in-situ and model estimates when available.

Compared to buoys, wind speed performance is about 1 m/s RMS, and wind direction RMS is typically 10 degrees for winds above 3 m/s. These comparisons were complicated by the often-strong surface currents and temperature gradients in our flight areas. For example, surface currents near the mouth of the Mississippi river in the Gulf of Mexico (see Figure 7) were over 1 m/s and the cold, fresh water in the plume was nearly five degrees Celsius cooler than the surrounding ocean water. During another flight in the Gulf of Mexico, a strong warm-core eddy drove 1 m/s currents and raised sea surface temperatures by four degrees Celsius compared to the surrounding ocean. DopplerScatt measurements responded to these perturbations in wind fields, and buoy comparisons required accounting for surface stability (due to temperature anomalies) and surface currents (which are fortunately also measured by DopplerScatt) for accurate results. This modulation is visible in Figure 7, where the Mississippi river plume has caused reduced wind speeds in DopplerScatt measurements due to the combination of cold water and strong currents flowing along the wind direction. An oil slick also led to a decrease in perceived wind speeds near the center-right of Figure 7, probably due to decreased backscatter in the presence of higher viscosity oil.

The validation of the current performance of DopplerScatt is more challenging due to the lack of available high-resolution synoptic current measurements. Rodriguez et al. [14] reported on qualitative comparisons against the Navy Coastal Ocean Model (NCOM), with significant agreement on the identification of frontal features. An additional experiment has been conducted in the Gulf of Mexico comparing ocean currents against those measured by Fugru's Remote Ocean Current Imaging System (ROCIS) (Rodriguez et al., 2019, unpublished Chevron report) showing high correlations and agreements on the current speed to better than 10 cm/s, although some direction differences could be observed at lower wind speeds, potentially caused by the two instruments measuring different depth currents. Detailed comparisons against HF radar data on the west coast of the United States is ongoing.

VII. Looking Forward

The future of Doppler Scatterometry looks promising. DopplerScatt will be flown as the primary instrument during the upcoming Submesoscale Ocean Dynamics Experiment (funded by NASA Earth Ventures Suborbital-3), which will survey small scale ocean currents to determine their roles in oceanic mixing, heat and nutrient transfer, and their interaction with the wind. S-MODE will generate many times the amount of data collected by DopplerScatt thus far and hopefully revolutionize our understanding of the submesoscale. Beyond the scientific data DopplerScatt produces, the instrument also acts as a technology development stepping stone to measuring vector ocean currents from space. With the National Academy's Decadal Review selection of vector ocean currents as a targeted climate observable to measure in the next ten years, and their suggestion of Doppler Scatterometry as the means, there is significant support for a spaceborne Doppler Scatterometer.

VIII. Conclusion

Doppler Scatterometery offers a powerful method for sensing submesoscale ocean vector winds and currents at synoptic scales. The DopplerScatt instrument has raised the technology readiness of essential technologies and algorithms to lay the foundation for a spaceborne winds and currents mission in the future. In the meantime, the high resolution and wide-swath synoptic views measured by DopplerScatt offer scientists unprecedented insight into the submesoscale regime.

Acknowledgment

This work was performed at the Jet Propulsion Laboratory, California Institute of Technology under contract with the National Aeronautics and Space Administration.

REFERENCES

[1] R. Ferrari and C. Wunsch, "Ocean Circulation Kinetic Energy: Reservoirs, Sources, and Sinks," *Annual Review of Fluid Mechanics*, vol. 41, pp. 253–282, 2009.

[2] M. Lévy, P. J. S. Franks, and K. S. Smith, "The role of submesoscale currents in structuring marine ecosystems," *Nature Communications*, vol. 9, p. 4758, 11 2018.

[3] A. G. Wineteer, "Towards Improved Estimates of Upper Ocean Energetics," 3 2016.

[4] J.-S. v. Storch, H. Sasaki, and J. Marotzke, "Wind-Generated Power Input to the Deep Ocean: An Estimate Using a 1/10 General Circulation Model," *Journal of Physical Oceanography*, vol. 37, pp. 657–672, 2007.

[5] N. A. of Sciences and Engineering, "Thriving on Our Changing Planet," 2018.

[6] K. A. Kelly, S. Dickinson, and G. C. Johnson, "Comparisons of Scatterometer and TAO Winds Reveal Time-Varying Surface Currents for the Tropical Pacific Ocean*," *Journal of Atmospheric and Oceanic Technology*, vol. 22, pp. 735–745, 6 2005.

[7] P. P. Sullivan and J. C. McWilliams, "Dynamics of Winds and Currents Coupled to Surface Waves," *Annual Review of Fluid Mechanics*, vol. 42, pp. 19–42, 2010.

[8] R. Small, S. deSzoeke, S. Xie, L. O'Neill, H. Seo, Q. Song, P. Cornillon, M. Spall, and S. Minobe, "Air–sea interaction over ocean fronts and eddies," *Dynamics of Atmospheres and Oceans*, vol. 45, 2008.

[9] D. B. Chelton, M. G. Schlax, M. H. Freilich, and R. F. Milliff, "Satellite measurements reveal persistent small-scale features in ocean winds," *Science*, vol. 303, no. 5660, pp. 978–983, 2 2004. [Online]. Available: https://doi.org/10.1126/science.1091901

[10] R. M. Goldstein and H. A. Zebker, "Interferometric radar measurement of ocean surface currents," *Nature*, vol. 328, p. 328707a0, 1987.

[11] R. Romeiser, H. Breit, M. Eineder, and H. Runge, "Demonstration of Current Measurements from Space by Along-Track SAR Interferometry with SRTM Data," *IEEE International Geoscience and Remote Sensing Symposium*, vol. 1, pp. 158–160, 2002.

[12] A. Freeman, V. Zlotnicki, T. Liu, B. Holt, R. Kwok, S. Yueh, JorgeVazquez, D. Siegel, and G. Lagerloef, "Ocean measurements from space in 2025," *Oceanography*, vol. 23, no. 4, pp. 144–161, 2010. [Online]. Available: http://www.jstor.org/stable/24860869

[13] B. Chapron, F. Collard, and F. Ardhuin, "Direct measurements of ocean surface velocity from space: Interpretation and validation," *Journal of Geophysical Research: Oceans (1978–2012)*, vol. 110, 2005.

[14] E. Rodríguez, A. Wineteer, D. Perkovic-Martin, T. Gál, B. Stiles, N. Niamsuwan, and R. Monje, "Estimating Ocean Vector Winds and Currents Using a Ka-Band Pencil-Beam Doppler Scatterometer," *Remote Sensing*, vol. 10, p. 576, 4 2018.

[15] Y. Y. Yurovsky, V. N. Kudryavtsev, S. A. Grodsky, and B. Chapron, "Ka-Band Dual Copolarized Empirical Model for the Sea Surface Radar Cross Section," *IEEE Transactions on Geoscience and Remote Sensing*, vol. 55, pp. 1629–1647, 2017.

[16] B. W. Stiles, B. D. Pollard, and R. S. Dunbar, "Direction Interval Retrieval With Thresholded Nudging: A Method for Improving the Accuracy of QuikSCAT Winds," *IEEE Transactions on Geoscience and Remote Sensing*, vol. 40, pp. 79–89, 2002.